OPEN ACCESS Freely available online

PLoS one

Noise Amplification in Human Tumor Suppression following Gamma Irradiation

Bo Liu[1,2], Shiwei Yan[1,3]*, Xingfa Gao[2]

1 Key Laboratory of Beam Technology and Material Modification of Ministry of Education, College of Nuclear Science and Technology, Beijing Normal University, Beijing, China, **2** Key Laboratory for Biomedical Effects of Nanomaterials and Nanosafety, Institute of High Energy Physics, Chinese Academy of Sciences, Beijing, China, **3** Beijing Radiation Center, Beijing, China

Abstract

The influence of noise on oscillatory motion is a subject of permanent interest, both for fundamental and practical reasons. Cells respond properly to external stimuli by using noisy systems. We have clarified the effect of intrinsic noise on the dynamics in the human cancer cells following gamma irradiation. It is shown that the large amplification and increasing mutual information with delay are due to coherence resonance. Furthermore, frequency domain analysis is used to study the mechanisms.

Citation: Liu B, Yan S, Gao X (2011) Noise Amplification in Human Tumor Suppression following Gamma Irradiation. PLoS ONE 6(8): e22487. doi:10.1371/journal.pone.0022487

Editor: Matjaz Perc, University of Maribor, Slovenia

Received May 12, 2011; **Accepted** June 22, 2011; **Published** August 5, 2011

Copyright: © 2011 Liu et al. This is an open-access article distributed under the terms of the Creative Commons Attribution License, which permits unrestricted use, distribution, and reproduction in any medium, provided the original author and source are credited.

Funding: SY acknowledges support from the National Natural Science Foundation of China under Grant No. 10975019, the Scientific Research Foundation for the Returned Overseas Chinese Scholars, Ministry of Personnel of China under Grant No. MOP2006138, and the Fundamental Research Funds for the Central Universities. The funders had no role in study design, data collection and analysis, decision to publish, or preparation of the manuscript.

Competing Interests: The authors have declared that no competing interests exist.

* E-mail: yansw@bnu.edu.cn

Introduction

How cells process noise is a challenging problem in illuminating the principle of intracellular motifs [1–3]. Shen-Orr *et al.* [4] find that much of a biological network is composed of repeated appearances of several highly significant motifs. Some network motifs have been used recently to explore the principle of cellular systems [4–6]. In two well-studied examples, the p53-Mdm2 regulatory network and the NF-κB signaling pathway, noisy oscillations in the cells following activation signals were studied in the experimental [7–12] and theoretical [13–31] aspects. The core circuit consists of one of the most common network designs, a negative feedback loop [32,33], where the active transcription factor promotes the transcription of its own repressor.

Mathematical models have achieved oscillatory dynamics by introducing *ad hoc* time delays to reproduce those that a system incurs when the various molecular components are manufactured [21,22,24,25,28,30,34–39]. Related works have been performed on many fields of research, where delays were found to play a central role. For example, the importance of delay has also recently been recognized in neuronal dynamics [40–43]. From the mathematical point of view, the difference between single-cell experiments and cell population experiments of simple regulatory networks arises from stochastic events in individual cells that are averaged out in cell population. As the noise intensity of the regulating species increases, the noise intensity of the regulated one also appears to increase. Noise can induce many phenomena in nonlinear dynamical systems, including stochastic resonance, coherence resonance, pattern formation and so on. Lots of original research [44–49] and review [50–52] articles have been devoted to the stochastic resonance phenomenon. Noise-induced patterns in semiconductor nanostructures have been recently investigated by means of theoretical models [53], where random fluctuations play an essential role. Our presented results are crucially relying on coherence resonance, which has been recently studied for temporal systems [54–57] and spatially extended systems [58–63]. Specifically the relevance of intrinsic noise was elaborated on periodic calcium waves in coupled cells [64] and spatial coherence resonance in excitable biochemical media [65] induced by internal noise. A recent comprehensive review [66] has been done on the stochastic coherence. The large amplification results from the existence of coherence resonance with delay and noise.

In this article, by exploiting a microscopical signal-response model which was proposed in our previous articles [37,38] for studying the dynamical mechanism of the oscillatory behaviors for the activities of p53 and Mdm2 proteins in individual cells, we will explore the mechanism of noise amplification by considering the stochastic events in the cells.

Results and Discussion

Noise amplification

We introduce the probability $Pr(n_P,n_M,t)$ for the p53 and Mdm2 populations $(P(t),M(t))=(n_P,n_M)$. Then the master equation for $Pr(n_P,n_M,t)$ is given by

$$\frac{dPr(n_P,n_M,t)}{dt}=\Pi(n_P,n_M)Pr(n_P,n_M,t)$$
$$+\alpha_M\sum_{m_P=0}^{\infty}\sum_{m_M=0}^{\infty}\frac{m_P^N}{K^N+m_P^N}(E_M^{-1}-1) \quad (1)$$
$$\times Pr(n_P,n_M,t;m_P,m_M,t-\tau),n_P,n_M=0\cdots\infty,$$

where τ is added to account for the time delay between the activation of p53 and the induction of Mdm2.

$Pr(n_P,n_M,t;m_P,m_M,t-\tau)$ is the joint probability distribution of having n_P p53 molecules, n_M Mdm2 molecules at time t and m_P p53 molecules, m_M Mdm2 molecules at time $t-\tau$. E_P and E_M are the unitary shift operators,

$$E_P Pr(n_P,n_M,t) = Pr(n_P+1,n_M,t),$$

$$E_M Pr(n_P,n_M,t) = Pr(n_P,n_M+1,t),$$

and

$$\begin{aligned}\Pi(n_P,n_M) = {} & S_P(E_P^{-1}-1) \\ & +[\alpha_P n_M(1-\gamma_P \mathcal{S}(t))+\mu_P](E_P-1)n_P \\ & +S_M(E_M^{-1}-1)+\mu_M(E_M-1)n_M.\end{aligned} \tag{2}$$

S_P, α_P, γ_P, μ_P, S_M, α_M, μ_M, K, N and $\mathcal{S}(t)$ are the parameters denoting various mechanisms as represented in our previous papers [37,38].

Assume that the time delay τ compared with other characteristic times of the system is large, so the processes at time t and $t-\tau$ are weakly correlated as $\Pr(n_P,n_M,t;m_P,t-\tau)=\Pr(n_P,n_M,t)\Pr(m_P,t-\tau)$. Adopting this approximation, we get

$$\begin{aligned}&\frac{dPr(n_P,n_M,t)}{dt} = \Pi(n_P,n_M)Pr(n_P,n_M,t) \\ &+\alpha_M\langle\frac{P^N(t-\tau)}{K^N+P^N(t-\tau)}\rangle(E_M^{-1}-1)Pr(n_P,n_M,t), n_P,n_M=0\cdots\infty.\end{aligned} \tag{3}$$

The generating function $G(s_1,s_2,t)$ is defined as

$$G(s_1,s_2,t) = \sum_{n_P,n_M=0}^{\infty} s_1^{n_P} s_2^{n_M} \Pr(n_P,n_M,t). \tag{4}$$

We convert the infinite set of ordinary differential equations (3) to a single partial differential equation for $G(s_1,s_2,t)$,

$$\begin{aligned}\frac{\partial G}{\partial t} = {} & (s_1-1)\left[S_P G(t)-\alpha_P s_2(1-\gamma_P\mathcal{S}(t))\frac{\partial^2 G(t)}{\partial s_1 \partial s_2}-\mu_P\frac{\partial G(t)}{\partial s_1}\right] \\ & +(s_2-1)\left[S_M G(t)-\mu_M\frac{\partial G(t)}{\partial s_2}+\alpha_M\langle\frac{P^N(t-\tau)}{K^N+P^N(t-\tau)}\rangle G(t)\right].\end{aligned} \tag{5}$$

The moments of the probability distribution can be found by expanding the generating function near $(s_1,s_2)=(1,1)$,

$$\begin{aligned}\left.\frac{\partial G}{\partial s_1}\right|_{\substack{s_1=1\\ s_2=1}} &= \left.\sum_{n_P,n_M=0}^{\infty} n_P s_1^{n_P-1} s_2^{n_M} \Pr(n_P,n_M,t)\right|_{\substack{s_1=1\\ s_2=1}} \\ &= \sum_{n_P=0}^{\infty} n_P \Pr(n_P,t) = \langle P(t)\rangle,\end{aligned} \tag{6}$$

$$\begin{aligned}\left.\frac{\partial G}{\partial s_2}\right|_{\substack{s_1=1\\ s_2=1}} &= \left.\sum_{n_P,n_M=0}^{\infty} n_M s_1^{n_P} s_2^{n_M-1} \Pr(n_P,n_M,t)\right|_{\substack{s_1=1\\ s_2=1}} \\ &= \sum_{n_M=0}^{\infty} n_M \Pr(n_M,t) = \langle M(t)\rangle,\end{aligned} \tag{7}$$

$$\begin{aligned}\left.\frac{\partial^2 G}{\partial s_1 \partial s_2}\right|_{\substack{s_1=1\\ s_2=1}} &= \left.\sum_{n_P,n_M=0}^{\infty} n_P n_M s_1^{n_P-1} s_2^{n_M-1} \Pr(n_P,n_M,t)\right|_{\substack{s_1=1\\ s_2=1}} \\ &= \sum_{n_P,n_M=0}^{\infty} n_P n_M \Pr(n_P,n_M,t) = \langle P(t)M(t)\rangle,\end{aligned} \tag{8}$$

$$\begin{aligned}\left.\frac{\partial^2 G}{\partial^2 s_1}\right|_{\substack{s_1=1\\ s_2=1}} &= \left.\sum_{n_P,n_M=0}^{\infty} n_P(n_P-1) s_1^{n_P-2} s_2^{n_M} \Pr(n_P,n_M,t)\right|_{\substack{s_1=1\\ s_2=1}} \\ &= \sum_{n_P=0}^{\infty} n_P(n_P-1)\Pr(n_P,t) = \langle P^2(t)\rangle - \langle P(t)\rangle,\end{aligned} \tag{9}$$

$$\begin{aligned}\left.\frac{\partial^2 G}{\partial^2 s_2}\right|_{\substack{s_1=1\\ s_2=1}} &= \left.\sum_{n_P,n_M=0}^{\infty} n_M(n_M-1) s_1^{n_P} s_2^{n_M-2} \Pr(n_P,n_M,t)\right|_{\substack{s_1=1\\ s_2=1}} \\ &= \sum_{n_M=0}^{\infty} n_M(n_M-1)\Pr(n_M,t) = \langle M^2(t)\rangle - \langle M(t)\rangle.\end{aligned} \tag{10}$$

Substituting the expansion

$$\begin{aligned}G(s_1-1,s_2-1,t) = {} & 1+(s_1-1)\alpha_1(t)+(s_2-1)\alpha_2(t)+\frac{1}{2}(s_1-1)^2 \\ & \beta_1(t)+\frac{1}{2}(s_2-1)^2\beta_2(t)+(s_1-1)(s_2-1) \\ & \beta_{12}(t)+\cdots\end{aligned} \tag{11}$$

into Eq. (5) we obtain

$$\frac{d\alpha_1}{dt} = S_P-\alpha_P(1-\gamma_P\mathcal{S}(t))\beta_{12}(t)-\mu_P\alpha_1(t), \tag{12a}$$

$$\frac{d\alpha_2}{dt} = S_M+\alpha_M\langle\frac{P^N(t-\tau)}{K^N+P^N(t-\tau)}\rangle-\mu_M\alpha_2(t), \tag{12b}$$

where the functions $\alpha_1(t)$, $\alpha_2(t)$ and $\beta_{12}(t)$ are Eqs. (6), (7) and (8), respectively. Above is the presentation of the derivation by help of generating functions. In fact, it delivers the same moment equations as the derivation by averaging the master equation. Both approaches run finally into equivalent approximations and problems if decoupling the moments. By the comparison between Eqs. (12) and the corresponding deterministic equations described in our previous papers [37,38], we find that due to

$$C(t) = \beta_{12}(t)-\alpha_1(t)\alpha_2(t), \tag{13a}$$

$$H(t-\tau) = \langle\frac{P^N(t-\tau)}{K^N+P^N(t-\tau)}\rangle-\frac{\langle P^N(t-\tau)\rangle}{K^N+\langle P^N(t-\tau)\rangle}, \tag{13b}$$

the limit cycle of the deterministic description [37,38] changes to a decaying scheme as shown in Fig. 1.

From our numerical results, the reason for the decaying can be considered as dephasing that is mainly caused by differences in the Hill function $P^N(t-\tau)/(K^N+P^N(t-\tau))$ between the cells. The reason that Hill functions are different is the different states of the different cells at time $t-\tau$, i.e., some dephasing happened at time $t-\tau$ for it to have this impact. The delay further amplifies the differences between cells, causing further dephasing. but if we take two cells with identical state space paths, their Hill functions will also be the same.

This initial difference between the particle numbers of chemical species in different cells, which causes the difference in Hill function at later time, is entirely caused by the intrinsic noise. In fact, any oscillating chemical system, with or without delayed dynamics, will demonstrate dephasing between different realizations, and it isn't an artifact of the delayed dynamics themselves, although this will undoubtedly cause further decorrelation of different realizations at later time, which causes the damped behavior at the population level (which can be thought of as simply taking a large number of realizations of the same stochastic system). Essentially, the value which the cell population converges to is simply approximately the mean of the invariant distribution of the chemical species for one cell, multiplied by the number of cells in the population of interest. This can be shown more rigorously for large populations using the ergodic property of the system.

Fig. 2 shows the average power spectrum $S_P(\omega)$ for $P(t)$ time series as a function of frequency ω. We also plot the spectrum of the corresponding deterministic model, with delay (e.g., time delay $\tau_d=100$ min in Fig. 2) but without noise, to compare its spectrum with stochastic ones. It can be clearly seen that $S_P(\omega)$ without noise is much smaller than those with noise. Significantly, for the cases with large τ (especially, τ is larger than the Hopf bifurcation point τ_c), there are obvious peaks appearing in $S_P(\omega)$ for $P(t)$ at $\omega\neq 0$. This tells us that there is a very large amplification of intrinsic noise due to the resonant effects. This characteristic phenomenon may be termed as coherence resonance with delay

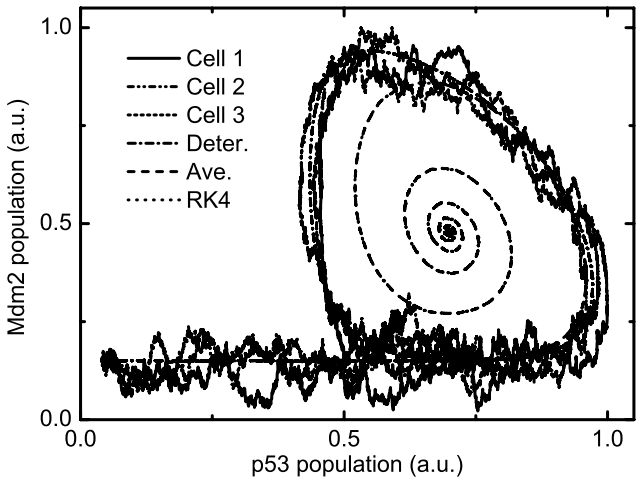

Figure 1. Normalized phase plot $(P(t),M(t))$ in 3 individual MCF7 cells following gamma irradiation, deterministic (Deter.) solutions $(P(t),M(t))$, and average (Ave.) populations $(\langle P(t)\rangle,\langle M(t)\rangle)$ in population of cells obtained with the exact DSSA (Ave.) and fourth-order Runge-Kutta (RK4) solutions of Eqs. (12) where the numerical values of $C(t)$ and $H(t-\tau)$ are obtained with the exact DSSA. The parameters are chosen as $S_P=0.5$ min^{-1}, $\alpha_P=1.8$ min^{-1}, $\gamma_P=0.996$, $\mu_P=2.5\times10^{-4}$ min^{-1}, $S_M=2.35\times10^{-3}$ min^{-1}, $\alpha_M=0.1$ min^{-1}, $\mu_M=0.05$ min^{-1}, $K=120$, $N=10$, $\tau=100$ min and $\tau_{th}>4000$ min.
doi:10.1371/journal.pone.0022487.g001

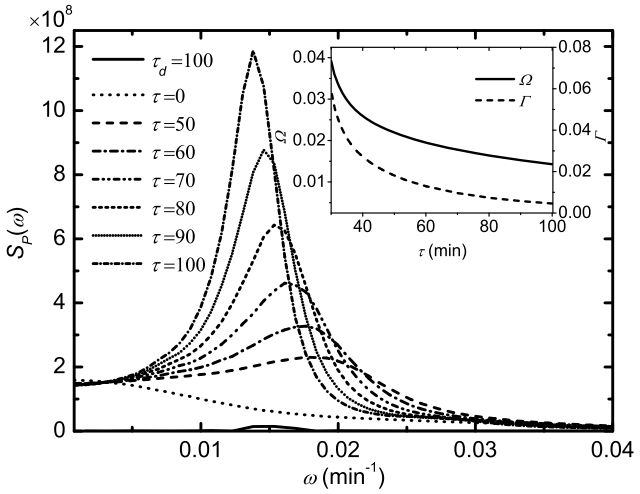

Figure 2. A plot of the average power spectrum $S_P(\omega)=\langle|\mathcal{F}[P(t)]|^2\rangle$ as a function of frequency ω with ($\tau=0,\cdots,100$ min) and without ($\tau_d=100$ min) noise, where $\mathcal{F}[P(t)]$ is Fourier transform of p53 dynamics from the time to the frequency domain, and the p53 dynamics $P(t)$ is obtained with the DSSA. Inset: Ω and Γ fitted with Eq. (14) vs. τ. The other parameters are as in Fig. 1.
doi:10.1371/journal.pone.0022487.g002

and noise, for distinguishing from the " stochastic resonance" in common sense.

The peak frequency corresponds to the characteristic frequency of the solution of Eqs. (12), which represents the mean frequency of Fourier transform $\mathcal{F}[P(t)]$. It is very intriguing that the width of $S_P(\omega)$ represents the dephasing effects, which gives the damping strength on the amplitude of $\langle P(t)\rangle$. In order to analyze this resonant oscillation more transparently, we phenomenologically fit $S_P(\omega)$ for the cases with large τ ($\tau>\tau_c$) shown in Fig. 2 by a formula

$$S_P(\omega)=\frac{\alpha+\beta\omega^2}{\left(\omega^2-\Omega^2\right)^2+\Gamma^2\omega^2}, \tag{14}$$

where the parameters α, β, Ω and Γ are τ-dependent. Note that Eq. (14) can be analytically derived with the chemical Langevin equations corresponding to Eqs. (1) under the linearization approximation.

The resultant Ω and Γ are shown in the inset picture of Fig. 2. It is obvious that the mean frequency Ω decreases against τ, which is consistent with the conclusion described in our previous article [37]. This is particularly important in biology because in general the low frequency is much more significant than higher frequency in biological systems. Γ also decreases as τ increasing, which means that the oscillation may dominate the evolution of $\langle P(t)\rangle$ and lasts for rather longer time for very large τ. This phenomenon is very intriguing from the biological point of view because it may tell us that the time delay induced by the underlying multistage reactions may weaken the effects of stochasticity and strengthen the oscillation of the relevant molecules.

Mutual information (MI) is meaningful to discuss resonant phenomena [67], so we give the mutual information between the two components p53 and Mdm2 in the nonlinear delayed-feedback network motif. MI is a measure of the amount of information that one random variable interacts with another. It is the reduction in the uncertainty of one random variable due to the

knowledge of the other [68]. MI between variables P and M can be represented as

$$MI(P,M)=H(P)+H(M)-H(P,M), \tag{15}$$

where the Shannon entropy, $H(P)$, $H(M)$, and the joint entropy $H(P,M)$ are defined as

$$H(P)=-\int \Pr(n_P)\log \Pr(n_P)dn_P, \tag{16a}$$

$$H(M)=-\int \Pr(n_M)\log \Pr(n_M)dn_M, \tag{16b}$$

$$H(P,M)=-\int\int \Pr(n_P,n_M)\log \Pr(n_P,n_M)dn_P n_M, \tag{16c}$$

where $\Pr(n_P)$ and $\Pr(n_M)$ are margin distribution functions and $\Pr(n_P,n_M)$ is the joint distribution function. Thus the MI can be represented as

$$MI(P,M)=\int\int \Pr(n_P,n_M)\log\frac{\Pr(n_P,n_M)}{\Pr(n_P)\Pr(n_M)}dn_P n_M. \tag{17}$$

MI is zero if and only if the two random variables are strictly independent [69]. Numerically calculating the mutual information between trajectories is in general a formidable task [70], since the joint distribution of continuous variable is smoothly obtained only for large scale stochastic simulation. Intensive work has been done on estimating the mutual information. Khan *et al.* [71] reviewed three MI estimators: Kernel density estimators, k-nearest neighbor method and Edgeworth expansion. Recently, Suzuki *et al.* [72] proposed a novel MI estimator called Least-Squares Mutual Information, and discussed the characteristics of the three existing approaches. However, it is accessible here due to the discreteness of the system with the exact delay stochastic simulation algorithm (DSSA) [73]. Information theory [74] provides a natural framework for many problems in biological information processing. The Shannon mutual information has been applied to study the stochastic resonance (SR) [67,75,76], instead of the signal-to-noise ratio (SNR). It can be seen from Fig. 3 that when the DNA is damaged, the phosphorylation of p53 modifies its binding properties to Mdm2, so MI is small; But when the signal is completely resolved, e.g., after $\tau_{th}=1750$ min, MI is large because the amount of p53 is kept low and tightly regulated by the genetic network of Mdm2 and p53 itself. Fig. 4 shows that MI in steady state increases with the increase of time delay due to the coherence resonance.

Fourier analysis

To describe the nonlinear dynamics more clearly, we use frequency domain analysis method to study the mechanisms of the p53 network motif. Our model can be described by a set of chemical Langevin equations corresponding to Eqs. (1),

$$\frac{dP(t)}{dt}=S_P-\alpha_P M(t)P(t)(1-\gamma_P \mathcal{S}(t)) -\mu_P P(t)+\eta_1(t), \tag{18a}$$

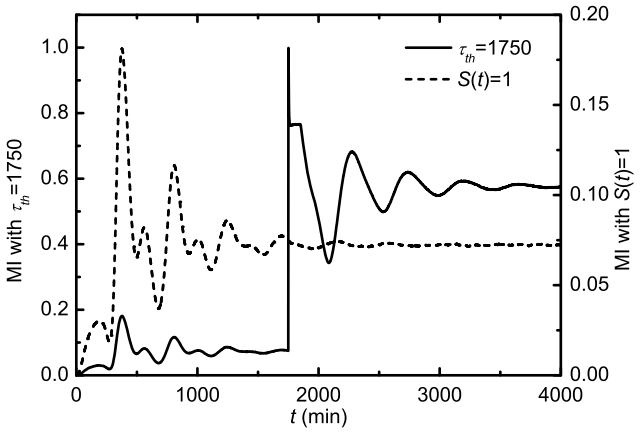

Figure 3. Evolution of Mutual information (MI) with $\tau_{th}=1750$ min and $\mathcal{S}(t)=1$. The other parameters are as in Fig. 1.
doi:10.1371/journal.pone.0022487.g003

$$\frac{dM(t)}{dt}=S_M+\alpha_M \Gamma(t)-\mu_M M(t)+\eta_2(t), \tag{18b}$$

where $\eta_1(t)$ and $\eta_2(t)$ are Gaussian white noise, $\langle\eta_i(t)\rangle=0$, $\langle\eta_i(t)\eta_j(t')\rangle=\langle\eta_i\eta_j\rangle\delta(t-t')$, $\{i,j=1,2\}$ [77].

In order to analyze our model in the frequency domain, we first replace $P(t)$ and $M(t)$ in Eqs. (18) by

$$P(t)=P^*+p(t), M(t)=M^*+m(t), \tag{19}$$

where P^* and M^* represent the stationary solutions of the deterministic equations of Eqs. (18) with $\tau=0$, which satisfy the equations

$$S_P-\alpha_P M^* P^*(1-\gamma_P)-\mu_P P^*=0, \tag{20a}$$

$$S_M+\alpha_M \Gamma(P^*)-\mu_M M^*=0. \tag{20b}$$

Since we are discussing the solution in the oscillatory scheme, here the signal $\mathcal{S}(t)$ is set to be 1. If one hopes to discuss the case of the

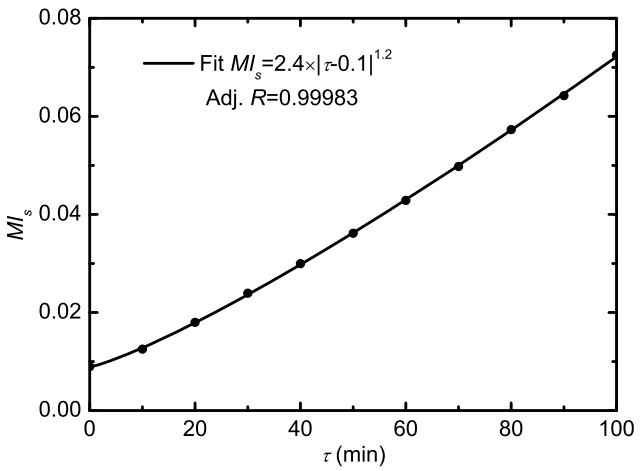

Figure 4. Mutual information (MI) in steady state as a function of time delay τ, where $MI_s=\lim_{t\to\infty} MI(P,M,t)$. The fit function and its adjusted R-Square are indicated. The parameters are as in Fig. 1.
doi:10.1371/journal.pone.0022487.g004

stationary solution in $t\to\infty$, he can simply set the parameter $\gamma_P\to 0$ mathematically, because at $t\to\infty$, the damage can be supposed to be completely resolved as $\mathcal{S}(t\to\infty)=0$, i.e., the signal $\mathcal{S}(t)$ is first set to 1, later γ_P is removed because $\mathcal{S}(t)$ is becoming 0 if time tends to infinity. Then Eqs. (18) can be rewritten as

$$\frac{dp}{dt}=Ap(t)+Bm(t)+Dp(t)m(t)+\eta_1(t), \tag{21a}$$

$$\frac{dm}{dt}=-\mu_M m(t)+Cp(t-\tau)+Ep^2(t-\tau)+\eta_2(t), \tag{21b}$$

where

$$A=-\alpha_P(1-\gamma_P)M^*-\mu_P, \tag{22a}$$

$$B=-\alpha_P(1-\gamma_P)P^*, \tag{22b}$$

$$C=\alpha_M\Gamma'(P^*), \tag{22c}$$

$$D=-\alpha_P(1-\gamma_P), \tag{22d}$$

$$E=\alpha_M\Gamma''(P^*)/2, \tag{22e}$$

and the nonlinear term is kept up to the second order in $p(t-\tau)$.

The Fourier transformations of Eqs. (18) take the form

$$i\omega p(\omega)=Ap(\omega)+Bm(\omega)+\frac{D}{\sqrt{2\pi}}F(\omega)+\eta_1(\omega), \tag{23a}$$

$$i\omega m(\omega)=-\mu_M m(\omega)+Ce^{-i\omega\tau}p(\omega)+\frac{Ee^{-i\omega\tau}}{\sqrt{2\pi}}G(\omega)+\eta_2(\omega), \tag{23b}$$

where

$$F(\omega)=\int_{-\infty}^{\infty}p(\omega-\omega_0)m(\omega_0)d\omega_0, \tag{24a}$$

$$G(\omega)=\int_{-\infty}^{\infty}p(\omega-\omega_0)p(\omega_0)d\omega_0. \tag{24b}$$

Since Eqs. (23) are integral equations, they can be solved by interpolation method and truncated at a specific order, the following calculation includes convolutions in the spectral presentation replacing the nonlinear items in the temporal one and truncating them, e.g., we can first solve the linear equation

$$i\omega p(\omega)=Ap(\omega)+Bm(\omega)+\eta_1(\omega), \tag{25a}$$

$$i\omega m(\omega)=-\mu_M m(\omega)+Ce^{-i\omega\tau}p(\omega)+\eta_2(\omega), \tag{25b}$$

substitute the solutions $p(\omega)$ and $m(\omega)$ of Eqs. (25) into Eqs. (24), and then $F(\omega)$ and $G(\omega)$ are functions of ω. Under the approximations of weak noise and weak negative feedback mechanism, in this paper, the solutions of both $p(\omega)$ and $m(\omega)$ are retained up to the second order of $\eta_1(\omega)$ and $\eta_2(\omega)$, because for Gaussian noise, the terms of higher order can be omitted in Ito-Wiener approximation. The validation of such approximations will be discussed with our numerical simulation later. We define

$$f_1(\omega)=i\omega+\mu_M, \tag{26a}$$

$$f_2(\omega)=Ce^{-i\omega\tau}, \tag{26b}$$

$$f_3(\omega)=i\omega-A-\frac{Bf_2(\omega)}{f_1(\omega)}, \tag{26c}$$

$$g_1(\omega)=\frac{1}{f_3(\omega)}, \tag{27a}$$

$$g_2(\omega)=\frac{B}{f_1(\omega)f_3(\omega)}, \tag{27b}$$

$$g_3(\omega)=\frac{1}{\sqrt{2\pi}f_3(\omega)}, \tag{27c}$$

$$g_4(\omega)=\frac{Df_2(\omega)}{f_1(\omega)}, \tag{27d}$$

$$g_5(\omega)=\frac{D}{f_1(\omega)}, \tag{27e}$$

$$g_6(\omega)=\frac{BEe^{-i\omega\tau}}{f_1(\omega)}, \tag{27f}$$

$$g_7(\omega)=\frac{Ee^{-i\omega\tau}f_3(\omega)}{f_2(\omega)}, \tag{27g}$$

and then it can be derived from Eqs. (23) that

$$p(\omega)=g_1(\omega)\eta_1(\omega)+g_2(\omega)\eta_2(\omega)+g_3(\omega)(DF(\omega)+g_6(\omega)G(\omega)), \tag{28a}$$

$$m(\omega)=\frac{f_2(\omega)}{f_1(\omega)}g_1(\omega)\eta_1(\omega)+\frac{f_2(\omega)g_2(\omega)+1}{f_1(\omega)}\eta_2(\omega)+g_3(\omega)\left[g_4(\omega)F(\omega)+\left(\frac{f_2(\omega)}{f_1(\omega)}+\frac{1}{\sqrt{2\pi}Bg_3(\omega)}\right)g_6(\omega)G(\omega)\right]. \tag{28b}$$

By defining the intermediate variables,

$$I_1(\omega,\omega_0)=(g_4(\omega_0)+g_6(\omega))g_1(\omega-\omega_0)g_1(\omega_0), \tag{29a}$$

$$I_2(\omega,\omega_0)=(g_2(\omega_0)g_4(\omega_0)+g_5(\omega_0)+g_2(\omega_0)g_6(\omega))g_1(\omega-\omega_0), \tag{29b}$$

$$I_3(\omega,\omega_0)=(g_4(\omega_0)+g_6(\omega))g_2(\omega-\omega_0)g_1(\omega_0), \tag{29c}$$

$$I_4(\omega,\omega_0)=(g_2(\omega_0)g_4(\omega_0)+g_5(\omega_0)+g_2(\omega_0)g_6(\omega))g_2(\omega-\omega_0), \tag{29d}$$

$$I_1'(\omega,\omega_0)=I_1(\omega,\omega_0)+g_7(\omega)g_1(\omega-\omega_0)g_1(\omega_0), \tag{30a}$$

$$I_2'(\omega,\omega_0)=I_2(\omega,\omega_0)+g_7(\omega)g_1(\omega-\omega_0)g_2(\omega_0), \tag{30b}$$

$$I_3'(\omega,\omega_0)=I_3(\omega,\omega_0)+g_7(\omega)g_2(\omega-\omega_0)g_1(\omega_0), \tag{30c}$$

$$I_4'(\omega,\omega_0)=I_4(\omega,\omega_0)+g_7(\omega)g_2(\omega-\omega_0)g_2(\omega_0), \tag{30d}$$

Eqs. (28) can be written as

$$\begin{aligned} p(\omega) &= g_1(\omega)\eta_1(\omega) + g_2(\omega)\eta_2(\omega) \\ &+ g_3(\omega)\Bigg(\int_{-\infty}^{\infty} I_1(\omega,\omega_0)\eta_1(\omega-\omega_0)\eta_1(\omega_0)d\omega_0 \\ &+ \int_{-\infty}^{\infty} I_2(\omega,\omega_0)\eta_1(\omega-\omega_0)\eta_2(\omega_0)d\omega_0 \\ &+ \int_{-\infty}^{\infty} I_3(\omega,\omega_0)\eta_2(\omega-\omega_0)\eta_1(\omega_0)d\omega_0 \\ &+ \int_{-\infty}^{\infty} I_4(\omega,\omega_0)\eta_2(\omega-\omega_0)\eta_2(\omega_0)d\omega_0\Bigg), \end{aligned} \tag{31a}$$

$$\begin{aligned} m(\omega) &= \frac{f_2(\omega)}{f_1(\omega)}g_1(\omega)\eta_1(\omega) + \frac{f_2(\omega)g_2(\omega)+1}{f_1(\omega)}\eta_2(\omega) \\ &+ \frac{f_2(\omega)}{f_1(\omega)}g_3(\omega)\Bigg(\int_{-\infty}^{\infty} I_1{}'(\omega,\omega_0)\eta_1(\omega-\omega_0)\eta_1(\omega_0)d\omega_0 \\ &+ \int_{-\infty}^{\infty} I_2{}'(\omega,\omega_0)\eta_1(\omega-\omega_0)\eta_2(\omega_0)d\omega_0 \\ &+ \int_{-\infty}^{\infty} I_3{}'(\omega,\omega_0)\eta_2(\omega-\omega_0)\eta_1(\omega_0)d\omega_0 \\ &+ \int_{-\infty}^{\infty} I_4{}'(\omega,\omega_0)\eta_2(\omega-\omega_0)\eta_2(\omega_0)d\omega_0\Bigg). \end{aligned} \tag{31b}$$

Let

$$J_k = \int_0^{\infty} I_k(0,\omega_0)d\omega_0, \tag{32a}$$

$$J_{m,n}(\omega) = \int_{-\infty}^{\infty} I_m(\omega,\omega_0)I_n^*(\omega,\omega_0)d\omega_0, \tag{32b}$$

$$L_{m,n}(\omega) = \int_{-\infty}^{\infty} I_m(\omega,\omega_0)I_n^*(\omega-\omega_0,\omega_0)d\omega_0, \tag{32c}$$

$$J_k' = \int_0^{\infty} I_k'(0,\omega_0)d\omega_0, \tag{33a}$$

$$J_{m,n}'(\omega) = \int_{-\infty}^{\infty} I_m'(\omega,\omega_0)I_n'^*(\omega,\omega_0)d\omega_0, \tag{33b}$$

$$L_{m,n}'(\omega) = \int_{-\infty}^{\infty} I_m'(\omega,\omega_0)I_n'^*(\omega-\omega_0,\omega_0)d\omega_0, \tag{33c}$$

where $\{k,m,n=1,2,3,4\}$. Then the correlation functions of $p(\omega)$ and $m(\omega)$ can be expressed as

$$\begin{aligned} S_p(\omega) &= \langle p(\omega)p^*(\omega')\rangle \\ &= \alpha_1\langle\eta_1^2\rangle + \alpha_2\langle\eta_1\eta_2\rangle + \alpha_3\langle\eta_2^2\rangle \\ &+ \alpha_4\langle\eta_1^2\rangle^2 + \alpha_5\langle\eta_2^2\rangle^2 + \alpha_6\langle\eta_1\eta_2\rangle^2 \\ &+ \alpha_7\langle\eta_1^2\rangle\langle\eta_1\eta_2\rangle + \alpha_8\langle\eta_1\eta_2\rangle\langle\eta_2^2\rangle, \end{aligned} \tag{34a}$$

$$\begin{aligned} S_m(\omega) &= \langle m(\omega)m^*(\omega')\rangle \\ &= \beta_1\langle\eta_1^2\rangle + \beta_2\langle\eta_1\eta_2\rangle + \beta_3\langle\eta_2^2\rangle \\ &+ \beta_4\langle\eta_1^2\rangle^2 + \beta_5\langle\eta_2^2\rangle^2 + \beta_6\langle\eta_1\eta_2\rangle^2 \\ &+ \beta_7\langle\eta_1^2\rangle\langle\eta_1\eta_2\rangle + \beta_8\langle\eta_1\eta_2\rangle\langle\eta_2^2\rangle. \end{aligned} \tag{34b}$$

The parameters α_1, β_1, α_2, β_2, $\cdots$, α_8, β_8 represent the contributions of $\langle\eta_1^2\rangle$, $\langle\eta_1\eta_2\rangle$, $\cdots$, $\langle\eta_1\eta_2\rangle\langle\eta_2^2\rangle$ to the correlation functions $S_p(\omega)$ and $S_m(\omega)$, respectively. With the aid of the intermediate variables, those parameters can be expressed as

$$\alpha_1(\omega) = |g_1(\omega)|^2, \tag{35}$$

$$\alpha_2(\omega) = 2\,\mathrm{Re}\left[g_1(\omega)g_2^*(\omega)\right], \tag{36}$$

$$\alpha_3(\omega) = |g_2(\omega)|^2, \tag{37}$$

$$\alpha_4(\omega) = 4|g_3(0)|^2J_1^2\delta(\omega) + |g_3(\omega)|^2(J_{1,1}(\omega) + L_{1,1}(\omega)), \tag{38}$$

$$\alpha_5(\omega) = 4|g_3(0)|^2J_4^2\delta(\omega) + |g_3(\omega)|^2(J_{4,4}(\omega) + L_{4,4}(\omega)), \tag{39}$$

$$\begin{aligned} \alpha_6(\omega) &= 4|g_3(0)|^2\left[J_2^2 + J_3^2 + 2(J_1J_4 + J_2J_3)\right]\delta(\omega) + |g_3(\omega)|^2 \\ &(J_{1,4}(\omega) + J_{4,1}(\omega) + J_{2,3}(\omega) + J_{3,2}(\omega) + J_{2,2}(\omega) + J_{3,3}(\omega) \\ &+ L_{1,4}(\omega) + L_{4,1}(\omega) + L_{2,3}(\omega) + L_{3,2}(\omega) + L_{2,2}(\omega) + L_{3,3}(\omega)), \end{aligned} \tag{40}$$

$$\begin{aligned} \alpha_7(\omega) &= 8|g_3(0)|^2(J_1J_2 + J_1J_3)\delta(\omega) + |g_3(\omega)|^2(J_{1,2}(\omega) + J_{2,1}(\omega) \\ &+ J_{1,3}(\omega) + J_{3,1}(\omega) + L_{1,2}(\omega) + L_{2,1}(\omega) + L_{1,3}(\omega) + L_{3,1}(\omega)), \end{aligned} \tag{41}$$

$$\begin{aligned} \alpha_8(\omega) &= 8|g_3(0)|^2(J_2J_4 + J_3J_4)\delta(\omega) + |g_3(\omega)|^2(J_{2,4}(\omega) + J_{4,2}(\omega) \\ &+ J_{3,4}(\omega) + J_{4,3}(\omega) + L_{2,4}(\omega) + L_{4,2}(\omega) + L_{3,4}(\omega) + L_{4,3}(\omega)), \end{aligned} \tag{42}$$

$$\beta_1(\omega) = \left|\frac{f_2(\omega)}{f_1(\omega)}\right|^2\alpha_1(\omega), \tag{43}$$

$$\beta_2(\omega) = \left|\frac{f_2(\omega)}{f_1(\omega)}\right|^2\alpha_2(\omega) + \frac{2\,\mathrm{Re}[f_2(\omega)g_1(\omega)]}{|f_1(\omega)|^2}, \tag{44}$$

$$\beta_3(\omega) = \left|\frac{f_2(\omega)}{f_1(\omega)}\right|^2\alpha_3(\omega) + \frac{2\,\mathrm{Re}[f_2(\omega)g_2(\omega)]+1}{|f_1(\omega)|^2}, \tag{45}$$

$$\beta_4(\omega) = \left|\frac{f_2(\omega)g_3(\omega)}{f_1(\omega)}\right|^2\left(4J_1'^2\delta(\omega) + J_{1,1}'(\omega) + L_{1,1}'(\omega)\right), \tag{46}$$

$$\beta_5(\omega) = \left|\frac{f_2(\omega)g_3(\omega)}{f_1(\omega)}\right|^2\left(4J_4'^2\delta(\omega) + J_{4,4}'(\omega) + L_{4,4}'(\omega)\right), \tag{47}$$

$$\begin{aligned} \beta_6(\omega) &= \left|\frac{f_2(\omega)g_3(\omega)}{f_1(\omega)}\right|^2\Big\{4\left[J_2'^2 + J_3'^2 + 2\left(J_1'J_4' + J_2'J_3'\right)\right]\delta(\omega) \\ &+ J_{1,4}'(\omega) + J_{4,1}'(\omega) + J_{2,3}'(\omega) + J_{3,2}'(\omega) + J_{2,2}'(\omega) + J_{3,3}'(\omega) \\ &+ L_{1,4}'(\omega) + L_{4,1}'(\omega) + L_{2,3}'(\omega) + L_{3,2}'(\omega) + L_{2,2}'(\omega) + L_{3,3}'(\omega)\Big\}, \end{aligned} \tag{48}$$

$$\beta_7(\omega)=\left|\frac{f_2(\omega)g_3(\omega)}{f_1(\omega)}\right|^2\Big[8\Big(J_1'J_2'+J_1'J_3'\Big)\delta(\omega)+J_{1,2}'(\omega)+J_{2,1}'(\omega)+J_{1,3}'(\omega)+J_{3,1}'(\omega)+L_{1,2}'(\omega)+L_{2,1}'(\omega)+L_{1,3}'(\omega)+L_{3,1}'(\omega)\Big], \tag{49}$$

$$\beta_8(\omega)=\left|\frac{f_2(\omega)g_3(\omega)}{f_1(\omega)}\right|^2\Big[8\Big(J_2'J_4'+J_3'J_4'\Big)\delta(\omega)+J_{2,4}'(\omega)+J_{4,2}'(\omega)+J_{3,4}'(\omega)+J_{4,3}'(\omega)+L_{2,4}'(\omega)+L_{4,2}'(\omega)+L_{3,4}'(\omega)+L_{4,3}'(\omega)\Big]. \tag{50}$$

With respect to

$$\begin{aligned}p(\omega)&=\frac{1}{\sqrt{2\pi}}\int_{-\infty}^{\infty}(P(t)-P^*)e^{-i\omega t}dt\\&=P(\omega)-\sqrt{2\pi}P^*\delta(\omega),\end{aligned} \tag{51a}$$

$$p^*(\omega')=P^*(\omega')-\sqrt{2\pi}P^*\delta^*(\omega'), \tag{51b}$$

Eqs. (34) can be read as

$$\begin{aligned}S_p(\omega)=&\langle P(\omega)P^*(\omega')\rangle+\sqrt{2\pi}P^{*2}\delta(\omega)\delta^*(\omega')\\&-\sqrt{2\pi}P^*[\langle P(\omega)\rangle\delta^*(\omega')+\langle P^*(\omega')\rangle\delta(\omega)],\end{aligned} \tag{52a}$$

$$\begin{aligned}S_m(\omega)=&\langle M(\omega)M^*(\omega')\rangle+\sqrt{2\pi}M^{*2}\delta(\omega)\delta^*(\omega')\\&-\sqrt{2\pi}M^*[\langle M(\omega)\rangle\delta^*(\omega')+\langle M^*(\omega')\rangle\delta(\omega)],\end{aligned} \tag{52b}$$

so the power spectra of $P(\omega)$ and $M(\omega)$ can be expanded from Eqs. (52) as

$$\begin{aligned}S_P(\omega)=\langle P(\omega)P^*(\omega')\rangle=&S_p(\omega)-\sqrt{2\pi}P^*\delta(\omega)\delta^*(\omega')\{P^*-g_3(\omega)\\&\Big[\langle\eta_1^2\rangle\int_{-\infty}^{\infty}I_1(\omega,\omega_0)d\omega_0+\langle\eta_2^2\rangle\int_{-\infty}^{\infty}I_4(\omega,\omega_0)d\omega_0\\&+\langle\eta_1\eta_2\rangle\int_{-\infty}^{\infty}(I_2(\omega,\omega_0)+I_3(\omega,\omega_0))d\omega_0\Big]-g_3^*(\omega')\\&\Big[\langle\eta_1^2\rangle\int_{-\infty}^{\infty}I_1^*(\omega',\omega_0)d\omega_0+\langle\eta_2^2\rangle\int_{-\infty}^{\infty}I_4^*(\omega',\omega_0)d\omega_0\\&+\langle\eta_1\eta_2\rangle\int_{-\infty}^{\infty}\big(I_2^*(\omega',\omega_0)+I_3^*(\omega',\omega_0)\big)d\omega_0\Big]\Big\},\end{aligned} \tag{53}$$

$$\begin{aligned}S_M(\omega)=\langle M(\omega)M^*(\omega')\rangle=&S_m(\omega)-\sqrt{2\pi}M^*\delta(\omega)\delta^*(\omega')\{M^*\\&-\frac{f_2(\omega)}{f_1(\omega)}g_3(\omega)\Big[\langle\eta_1^2\rangle\int_{-\infty}^{\infty}I_1'(\omega,\omega_0)d\omega_0+\langle\eta_2^2\rangle\\&\int_{-\infty}^{\infty}I_4'(\omega,\omega_0)d\omega_0+\langle\eta_1\eta_2\rangle\int_{-\infty}^{\infty}\Big(I_2'(\omega,\omega_0)+I_3'(\omega,\omega_0)\Big)d\omega_0\Big]\\&-\frac{f_2^*(\omega')}{f_1^*(\omega')}g_3^*(\omega')\Big[\langle\eta_1^2\rangle\int_{-\infty}^{\infty}I_1'^*(\omega',\omega_0)d\omega_0+\langle\eta_2^2\rangle\\&\int_{-\infty}^{\infty}I_4'^*(\omega',\omega_0)d\omega_0+\langle\eta_1\eta_2\rangle\int_{-\infty}^{\infty}\Big(I_2'^*(\omega',\omega_0)+I_3'^*(\omega',\omega_0)\Big)d\omega_0\Big]\}.\end{aligned} \tag{54}$$

If we remove the nonlinear terms in Eqs. (21), Eqs. (34) become

$$S_p(\omega)=\frac{(\omega^2+\mu_M^2)\langle\eta_1^2\rangle+2B\mu_M\langle\eta_1\eta_2\rangle+B^2\langle\eta_2^2\rangle}{(\omega^2+A\mu_M+BC\cos\omega\tau)^2+[\omega(\mu_M-A)+BC\sin\omega\tau]^2}, \tag{55a}$$

$$S_m(\omega)=\frac{C^2\langle\eta_1^2\rangle-2C(\omega\sin\omega\tau+A\cos\omega\tau)\langle\eta_1\eta_2\rangle+(\omega^2+A^2)\langle\eta_2^2\rangle}{(\omega^2+A\mu_M+BC\cos\omega\tau)^2+[\omega(\mu_M-A)+BC\sin\omega\tau]^2}. \tag{55b}$$

When τ is small, an approximation can be made,

$$\sin\omega\tau\approx\omega\tau, \tag{56a}$$

$$\cos\omega\tau\approx1-\frac{(\omega\tau)^2}{2}, \tag{56b}$$

and then Eqs. (55) become

$$S_f(\omega)=\langle|f(\omega)|^2\rangle=\frac{\alpha_f+\beta_f\omega^2}{\left(\omega^2+\Omega^2\right)^2+\Gamma^2\omega^2},\{f=p,m\}, \tag{57}$$

where

$$\Omega=\left(\frac{A\mu_M+BC}{\tau^2BC/2-1}\right)^2, \tag{58}$$

$$\Gamma=\frac{\mu_M-A+\tau BC}{1-\tau^2BC/2}. \tag{59}$$

For $S_p(\omega)$,

$$\alpha_p=\frac{\mu_M^2\langle\eta_1^2\rangle+2B\mu_M\langle\eta_1\eta_2\rangle+B^2\langle\eta_2^2\rangle}{1-\tau^2BC/2}, \tag{60a}$$

$$\beta_p=\frac{\langle\eta_1^2\rangle}{(1-\tau^2BC/2)^2}. \tag{60b}$$

For $S_m(\omega)$,

$$\alpha_m=\frac{C^2\langle\eta_1^2\rangle-2AC\langle\eta_1\eta_2\rangle+A^2\langle\eta_2^2\rangle}{(1-\tau^2BC/2)^2}, \tag{61a}$$

$$\beta_m=\frac{\tau C(A\tau-2)\langle\eta_1\eta_2\rangle+\langle\eta_2^2\rangle}{(1-\tau^2BC/2)^2}. \tag{61b}$$

It is worthwhile to mention that a module, which consists of two components, has been discussed recently [78]. They studied a set of coupled Langevin equations for the interacting species. It is very interesting that in the absence of delay and nonlinearity, i.e., a special case of the spectrum as $\tau=0$ in Eqs. (55), Eqs. (34) can be

reduced as

$$S_p(\omega)=\frac{\left(\mu_M^2+\omega^2\right)\langle\eta_1^2\rangle+2B\mu_M\langle\eta_1\eta_2\rangle+B^2\langle\eta_2^2\rangle}{\left(A\mu_M+BC\right)^2+\left(A^2+2BC+\mu_M^2\right)\omega^2+\omega^4}, \quad (62a)$$

$$S_m(\omega)=\frac{C^2\langle\eta_1^2\rangle-2AC\langle\eta_1\eta_2\rangle+\left(A^2+\omega^2\right)\langle\eta_2^2\rangle}{\left(A\mu_M+BC\right)^2+\left(A^2+2BC+\mu_M^2\right)\omega^2+\omega^4}, \quad (62b)$$

which are consistent with the results presented in the previous paper [78].

Another characteristic feature of Eqs. (34) is that when $\langle\eta_1\eta_2\rangle$ is assumed to be zero, which means that η_1 and η_2 are uncorrelated, both $S_p(\omega)$ and $S_m(\omega)$ can be written as a sum of two contributions which is the so-called spectral addition rule as derived in the previous paper [78]. Even in this case, the coefficients in our results still include the effects coming from the time delay and negative feedback mechanism.

In our numerical calculation, we use the fourth-order stochastic Runge-Kutta method for integrating the chemical Langevin equations (18), and Gaussian integration method to calculate the integrations in Eqs. (34). The numerical results have shown that the correlation functions $S_p(\omega)$ and $S_m(\omega)$ for $p(t)$ and $m(t)$ are precisely consistent between the ones with chemical Langevin equations (18) and the ones with Eqs. (34), which verifies our truncation method in Eqs. (23). The Fourier transforms of p53 and Mdm2 dynamics show that the number of the resonant peaks would increase as time delay increases, which is consistent with the experimental results [12]. The general finding of our analysis is that an increase of delay between activation and induction induces an oscillatory behavior with frequency which corresponds nearly to the delay time. The spectral analysis as well as the mutual information supports this finding. The general finding is in good agreement with our previous work [37].

Bioscience and nanoscience provide pretty examples of nonequilibrium and nonlinear dynamics in which noise can be expected to have unavoidable effects. The methods developed over years to deal with the effects in physical systems will help us to further our understanding of the mechanisms ascribed to nonlinearity and noise.

Methods

The stochastic p53 circuit was characterized by a Monte Carlo method called the exact DSSA. Numerical integration of the equations was carried out using Matlab software.

Acknowledgments

Thanks are going to Yizhao Geng for a critical reading of the manuscript. We acknowledge the fruitful comments of the unknown referee which helped a lot to improve the present publication.

Author Contributions

Conceived and designed the experiments: BL SY. Performed the experiments: BL. Analyzed the data: BL SY. Contributed reagents/materials/analysis tools: BL SY XG. Wrote the paper: BL SY XG.

References

1. Shibata T, Fujimoto K (2005) Noisy signal amplification in ultrasensitive signal transduction. Proceedings of the National Academy of Sciences of the United States of America 102: 331–336.
2. Samoilov M, Plyasunov S, Arkin AP (2005) Stochastic amplification and signaling in enzymatic futile cycles through noise-induced bistability with oscillations. Proceedings of the National Academy of Sciences of the United States of America 102: 2310–2315.
3. Detwiler PB, Ramanathan S, Sengupta A, Shraiman BI (2000) Engineering aspects of enzymatic signal transduction: Photoreceptors in the retina. Biophysical Journal 79: 2801–2817.
4. Shen-Orr SS, Milo R, Mangan S, Alon U (2002) Network motifs in the transcriptional regulation network of escherichia coli. Nature Genetics 31: 64–68.
5. Yeger-Lotem E, Sattath S, Kashtan N, Itzkovitz S, Milo R, et al. (2004) Network motifs in integrated cellular networks of transcription-regulation and protein-protein interaction. Proceedings of the National Academy of Sciences of the United States of America 101: 5934–5939.
6. Milo R, Shen-Orr S, Itzkovitz S, Kashtan N, Chklovskii D, et al. (2002) Network motifs: Simple building blocks of complex networks. Science 298: 824–827.
7. Haupt Y, Maya R, Kazaz A, Oren M (1997) Mdm2 promotes the rapid degradation of p53. Nature 387: 296–299.
8. Kubbutat MHG, Jones SN, Vousden KH (1997) Regulation of p53 stability by mdm2. Nature 387: 299–303.
9. Bar-Or RL, Maya R, Segel LA, Alon U, Levine AJ, et al. (2000) Generation of oscillations by the p53-mdm2 feedback loop: A theoretical and experimental study. Proceedings of the National Academy of Sciences of the United States of America 97: 11250–11255.
10. Lahav G, Rosenfeld N, Sigal A, Geva-Zatorsky N, Levine AJ, et al. (2004) Dynamics of the p53- mdm2 feedback loop in individual cells. Nature Genetics 36: 147–150.
11. Geva-Zatorsky N, Rosenfeld N, Itzkovitz S, Milo R, Sigal A, et al. (2006) Oscillations and variability in the p53 system. Molecular Systems Biology 2: 2006.0033.
12. Geva-Zatorsky N, Dekel E, Batchelor E, Lahav G, Alon U (2010) Fourier analysis and systems identification of the p53 feedback loop. Proceedings of the National Academy of Sciences of the United States of America 107: 13550–13555.
13. Hofseth LJ, Hussain SP, Harris CC (2004) p53: 25 years after its discovery. Trends in Pharmacological Sciences 25: 177–181.
14. Bray D (1995) Protein molecules as computational elements in living cells. Nature 376: 307–312.
15. Ferrell Jr. JE, Xiong W (2001) Bistability in cell signaling: How to make continuous processes discontinuous, and reversible processes irreversible. Chaos: An Interdisciplinary Journal of Nonlinear Science 11: 227–236.
16. Tyson JJ (2004) Monitoring p53's pulse. Nature Genetics 36: 113–114.
17. Tyson JJ (2006) Another turn for p53. Molecular Systems Biology 2: 2006.0032.
18. Batchelor E, Mock CS, Bhan I, Loewer A, Lahav G (2008) Recurrent initiation: A mechanism for triggering p53 pulses in response to dna damage. Molecular Cell 30: 277–289.
19. Wilkinson DJ (2009) Stochastic modelling for quantitative description of heterogeneous biological systems. Nature Reviews Genetics 10: 122–133.
20. Batchelor E, Loewer A, Lahav G (2009) The ups and downs of p53: understanding protein dynamics in single cells. Nature Reviews Cancer 9: 371–377.
21. Tiana G, Jensen MH, Sneppen K (2002) Time delay as a key to apoptosis induction in the p53 network. The European Physical Journal B - Condensed Matter and Complex Systems 29: 135–140.
22. Mihalas GI, Simon Z, Balea G, Popa E (2000) Possible oscillatory behavior in p53-mdm2 interaction computer simulation. Journal of Biological Systems 8: 21–29.
23. Nelson DE, Ihekwaba AEC, Elliott M, Johnson JR, Gibney CA, et al. (2004) Oscillations in nf-κb signaling control the dynamics of gene expression. Science 306: 704–708.
24. Puszynski K, Hat B, Lipniacki T (2008) Oscillations and bistability in the stochastic model of p53 regulation. Journal of Theoretical Biology 254: 452–465.
25. Proctor C, Gray D (2008) Explaining oscillations and variability in the p53-mdm2 system. BMC Systems Biology 2: 75.
26. Sun T, Chen C, Wu Y, Zhang S, Cui J, et al. (2009) Modeling the role of p53 pulses in dna damage-induced cell death decision. BMC Bioinformatics 10: 190.
27. Zhang X, Liu F, Cheng Z, Wang W (2009) Cell fate decision mediated by p53 pulses. Proceedings of the National Academy of Sciences of the United States of America 106: 12245–12250.
28. Cai X, Yuan Z (2009) Stochastic modeling and simulation of the p53-mdm2/mdmx loop. Journal of Computational Biology 16: 917–933.
29. Abou-Jaoude W, Ouattara DA, Kaufman M (2009) From structure to dynamics: Frequency tuning in the p53-mdm2 network i. logical approach. Journal of Theoretical Biology 258: 561–577.
30. Ouattara DA, Abou-Jaoude W, Kaufman M (2010) From structure to dynamics: Frequency tuning in the p53-mdm2 network. ii differential and stochastic approaches. Journal of Theoretical Biology 264: 1177–1189.
31. Hunziker A, Jensen M, Krishna S (2010) Stress-specific response of the p53-mdm2 feedback loop. BMC Systems Biology 4: 94.

32. Stricker J, Cookson S, Bennett MR, Mather WH, Tsimring LS, et al. (2008) A fast, robust and tunable synthetic gene oscillator. Nature 456: 516–519.
33. Danino T, Mondragon-Palomino O, Tsimring L, Hasty J (2010) A synchronized quorum of genetic clocks. Nature 463: 326–330.
34. Ma L, Wagner J, Rice JJ, Hu W, Levine AJ, et al. (2005) A plausible model for the digital response of p53 to dna damage. Proceedings of the National Academy of Sciences of the United States of America 102: 14266–14271.
35. Monk NAM (2003) Oscillatory expression of hes1, p53, and nf-κb driven by transcriptional time delays. Current Biology 13: 1409–1413.
36. Barrio M, Burrage K, Leier A, Tian T (2006) Oscillatory regulation of hes1: Discrete stochastic delay modelling and simulation. PLoS Computational Biology 2: 1017–1030.
37. Yan S, Zhuo Y (2006) A unified model for studying dna damage-induced p53-mdm2 interaction. Physica D: Nonlinear Phenomena 220: 157–162.
38. Yan S (2007) Negative feedback dynamics and oscillatory activities in regulatory biological networks. Journal of Biological Systems 15: 123–138.
39. Schlicht R, Winkler G (2008) A delay stochastic process with applications in molecular biology. Journal of Mathematical Biology 57: 613–648.
40. Wang Q, Perc M, Duan Z, Chen G (2009) Delay-induced multiple stochastic resonances on scalefree neuronal networks. Chaos: An Interdisciplinary Journal of Nonlinear Science 19: 023112.
41. Wang Q, Perc M, Duan Z, Chen G (2009) Synchronization transitions on scale-free neuronal networks due to finite information transmission delays. Physical Review E 80: 026206.
42. Wang Q, Duan Z, Perc M, Chen G (2008) Synchronization transitions on small-world neuronal networks: Effects of information transmission delay and rewiring probability. Europhysics Letters 83: 50008.
43. Wang Q, Chen G, Perc M (2011) Synchronous bursts on scale-free neuronal networks with attractive and repulsive coupling. PLoS ONE 6: e15851.
44. Nicolis C, Nicolis G (1981) Stochastic aspects of climatic transitions-additive fluctuations. Tellus 33: 225–234.
45. Benzi R, Sutera A, Vulpiani A (1981) The mechanism of stochastic resonance. Journal of Physics A: Mathematical and General 14: L453–L457.
46. Longtin A (1997) Autonomous stochastic resonance in bursting neurons. Physical Review E 55: 868–876.
47. Yeung MKS, Strogatz SH (1999) Time delay in the kuramoto model of coupled oscillators. Physical Review Letters 82: 648–651.
48. Kim S, Park SH, Pyo HB (1999) Stochastic resonance in coupled oscillator systems with time delay. Physical Review Letters 82: 1620–1623.
49. Ohira T, Sato Y (1999) Resonance with noise and delay. Physical Review Letters 82: 2811–2815.
50. Gammaitoni L, Hanggi P, Jung P, Marchesoni F (1998) Stochastic resonance. Reviews of Modern Physics 70: 223–287.
51. Lindner B, Garcia-Ojalvo J, Neiman A, Schimansky-Geier L (2004) Effects of noise in excitable systems. Physics Reports 392: 321–424.
52. McDonnell MD, Abbott D (2009) What is stochastic resonance? definitions, misconceptions, debates, and its relevance to biology. PLoS Computational Biology 5: e1000348.
53. Stegemann G, Balanov AG, Scholl E (2005) Noise-induced pattern formation in a semiconductor nanostructure. Physical Review E 71: 016221.
54. Sigeti D, Horsthemke W (1989) Pseudo-regular oscillations induced by external noise. Journal of Statistical Physics 54: 1217–1222.
55. Hu G (1993) Stochastic resonance without external periodic force. Physical Review Letters 71: 807–810.
56. Rappel WJ, Strogatz SH (1994) Stochastic resonance in an autonomous system with a nonuniform limit cycle. Physical Review E 50: 3249–3250.
57. Pikovsky AS, Kurths J (1997) Coherence resonance in a noise-driven excitable system. Physical Review Letters 78: 775–778.
58. Carrillo O, Santos MA, Garca-Ojalvo J, Sancho JM (2004) Spatial coherence resonance near pattern-forming instabilities. Europhysics Letters 65: 452–458.
59. Perc M (2005) Noise-induced spatial periodicity in excitable chemical media. Chemical Physics Letters 410: 49–53.
60. Perc M (2005) Spatial coherence resonance in excitable media. Physical Review E 72: 016207.
61. Perc M, Marhl M (2006) Minimal model for spatial coherence resonance. Physical Review E 73: 066205.
62. Perc M (2005) Spatial decoherence induced by small-world connectivity in excitable media. New Journal of Physics 7: 252.
63. Sun X, Perc M, Lu Q, Kurths J (2008) Spatial coherence resonance on diffusive and small-world networks of hodgkin-huxley neurons. Chaos: An Interdisciplinary Journal of Nonlinear Science 18: 023102.
64. Perc M, Gosak M, Marhl M (2007) Periodic calcium waves in coupled cells induced by internal noise. Chemical Physics Letters 437: 143–147.
65. Gosak M, Marhl M, Perc M (2007) Spatial coherence resonance in excitable biochemical media induced by internal noise. Biophysical Chemistry 128: 210–214.
66. Sagues F, Sancho JM, Garcia-Ojalvo J (2007) Spatiotemporal order out of noise. Reviews of Modern Physics 79: 829–882.
67. Munakata T, Sato AH, Hada T (2005) Stochastic resonance in a simple threshold system from a static mutual information point of view. Journal of the Physical Society of Japan 74: 2094–2098.
68. Cover TM, Thomas JA (1991) Elements of Information Theory. New York: Wiley.
69. Kraskov A, Stogbauer H, Grassberger P (2004) Estimating mutual information. Physical Review E 69: 066138.
70. Tostevin F, Ten Wolde PR (2009) Mutual information between input and output trajectories of biochemical networks. Physical Review Letters 102: 218101.
71. Khan S, Bandyopadhyay S, Ganguly AR, Saigal S, Erickson DJ, et al. (2007) Relative performance of mutual information estimation methods for quantifying the dependence among short and noisy data. Physical Review E 76: 026209.
72. Suzuki T, Sugiyama M, Kanamori T, Sese J (2009) Mutual information estimation reveals global associations between stimuli and biological processes. BMC Bioinformatics 10: S52.
73. Cai X (2007) Exact stochastic simulation of coupled chemical reactions with delays. The Jounal of Chemical Physics 126: 124108.
74. Shannon CE (1949) Communication in the presence of noise. Proceedings of the IRE 37: 10–21.
75. Munakata T, Kamiyabu M (2006) Stochastic resonance in the fitzhugh-nagumo model from a dynamic mutual information point of view. The European Physical Journal B - Condensed Matter and Complex Systems 53: 239–243.
76. Bulsara AR, Zador A (1996) Threshold detection of wideband signals: A noise-induced maximum in the mutual information. Physical Review E 54: R2185–R2188.
77. Risken H (1989) The Fokker-Plank Equation: Methods of Solution and Applications. Berlin: Springer.
78. Tanase-Nicola S, Warren PB, Ten Wolde PR (2006) Signal detection, modularity, and the correlation between extrinsic and intrinsic noise in biochemical networks. Physical Review Letters 97: 068102.